

# Development of Sustainable CNT-polymer Conductive Ink

Jhunjhun Kumar Mishra\*, Vishal Francis

Department of Mechanical Engineering, Lovely Professional University, Phagwara, Punjab, India. \*Corresponding Author's Email: msku1995@gmail.com

## Abstract

Additive manufacturing (AM) in the running scenarios is highly recommendable mode of production of electronics applications within industries; Direct ink writing (DIW) is one of most applications procedures of AM to print the solvent-based ink to complex geometry in 3D printing. The main objective of this research to develop a Carbon-formed conductive ink which is more biodegradable, conductive, electrically conducting, ideal rheological, structural and thermal behavior to develop an ink that can be extruded with precision and behaves post-print stability. In this research, multi-walled CNTs are the conductive filler and corn-starch and polyvinyl alcohol (PVA) are the biodegradable binders that increase dispersion, flexibility and mechanical strength. To enhance ink homogeneity and ink flow, ethylene glycol and Triton X-100 are added. Taguchi method is used to determine the best compositional ratios in terms of wt %, to maintain balanced rheological viscosity. The Fourier Transform Infrared Spectroscopy (FTIR), X-ray diffraction (XRD), Scanning Electron Microscopy (SEM), Thermogravimetric Analysis (TGA) and Electrochemical Workstation Metrohm characterisations are used to determine the relationship between microstructural uniformity and thermal stability and print performance. The optimized ink has consistently high rheological stability (86.9 Pa·s), which allows easy DIW printing of homogeneous and adherent layers. Based on Taguchi suggested composition of conductive ink 3D printing is done where different critical geometry has printed successfully. This research developed a plausible path toward eco-friendly carbon-formed conductive ink, which will aid in the making of 3D printing solutions permitting more friendly and dependable use in preparing flexible sensors and other electronics applications.

**Keywords:** Additive Manufacturing, Conductive Ink, Corn-Starch, Direct Ink Writing, Sustainable Ink.

## Introduction

Direct ink writing (DIW) is under intensive research with the use of conductive inks to develop and deploy increased methods of unique electronics, printed sensors and embedded circuits. Carbon nanotubes (CNTs) have been one of the most popular conductive fillers of great interest because of their high aspect ratio, excellent electrical conductivity and mechanical flexibility. The previous research has shown that CNT-based inks are able to reach electrical conductivities between  $10^{-2}$  to  $10^1$  S·cm<sup>-1</sup>, as a result of filler concentration, dispersion quality and choice of polymeric binders (1). Most of these formulations, however, demand relatively large CNT loadings in order to achieve electrical percolation, which effectively undermines the ink printability and long-term rheological stability (2). Rheologically, DIW inks have to meet a broad operating range to extrude in a continuous fashion, be shape faithful and be dimensionally precise. The

past studies have revealed that printable conductive inks usually have low-shear viscosities of 30 to 70 Pa·s and have a strong tendency to shear thin to pass through fine nozzles (3). Inks developed at frequencies lower than this are also likely to experience filament spreading and poor layer stacking and systems above 100 Pa·s are also likely to experience nozzle clogging, non-uniform extrusion and high printing pressures (4). These limitations manifest a fatal trade-off between electrical functionality and the rheological appropriateness of current CNT-based DIW inks. The environmental concerns also curtail the style of most of the reported conductive inks. A number of the previous formulations depend on organic solvents, non-biodegradable polymers, or surfactants that are not very green for the environment, which brings into question volatile organic compound emissions, safety of the operators and recycling (5). Therefore, the

This is an Open Access article distributed under the terms of the Creative Commons Attribution CC BY license (<http://creativecommons.org/licenses/by/4.0/>), which permits unrestricted reuse, distribution and reproduction in any medium, provided the original work is properly cited.

(Received 26<sup>th</sup> October 2025; Accepted 06<sup>th</sup> March 2026; Published 01<sup>st</sup> April 2026)

challenge of designing conductive inks that are simultaneously conductive, stable to be printed and made environmentally more eco-friendly has not been successfully addressed in the DIW research (6).

In this regard, the current work presents a sustainable CNT polymer conductive ink that would help eliminate the issues above. This proposed formulation also exhibits a significant improvement in the electrical conductivity at low CNT loading and hence percolation is possible without being overloaded with fillers. This enhancement implies one order of magnitude in terms of conductivity against a few other water-based CNT inks at similar filler densities reported in the past (7, 8). At the same time, the ink has a wider and more consistent rheological window of 80-90 Pa-s, that provides a stable extrusion, good shape maintenance and fewer flow instabilities during DIW.

Notably, the formulation uses a water-based polymer backbone and a green solvent co-solvent that produces minimal co-solvent toxicity as well as enhances biodegradability compared to solvent-based conductive inks that were previously reported (9). This study makes contributions towards the functionality and sustainability of CNT-based inks, which are utilized in DIW in terms of balancing the conductivity capacity, optimal rheology and environmental impact. This produced ink formulation can thus offer an expedient and scalable route to next-generation printed electronics with better reliability of

processing performance and environmental friendliness.

The latest studies summarized in Table 1 focus on dispersion and fundamental rheology for various printing techniques, yet seldom integrate (a) genuinely eco-sustainable, renewable binders (e.g., corn starch), (b) DIW-specific rheology optimization and (c) a formal statistical optimization approach like Taguchi. Additionally, DIW-specific conductivity vs extrusion fidelity trade-offs and comprehensive post-print microstructure-property correlations are insufficiently addressed across the surveyed works (10). To fill the identified gaps, the present study develops and optimizes a CNT/corn-starch/PVA ink tailored for DIW by (a) systematically formulating multiple wt % compositions, (b) applying Taguchi method to determine an optimal composition balancing viscosity and (c) performing full physicochemical and post-print characterization (FTIR, XRD, SEM and TGA) to establish microstructure-property relationships for printed geometries. This approach intentionally prioritizes renewable binder usage (corn-starch) and water-compatible processing to advance green, extrusion-based printed electronics while benchmarking performance against recent literature findings (11). The next section of this research study will be following as Materials and Methods (will detail materials, ink formulation table, sample designs, Taguchi methods and the DIW printing/characterization workflow), next results and discussion and then conclusion.

**Table 1:** Comparative Overview of Conductive Ink Formulations and Processing Strategies Reported in Previous Studies and the Present Work

Year	Material System	Printing Technique	Water-Based	Biodegradable Binder	Electrical Conductivity	Rheological Optimization	References
2025	DIW multiphase particle systems	DIW	Partial	X	✓	✓	(1)
2021	UV-curable nano-silver ink	Screen printing	X	X	✓	✓	(2)
2019	Conductive nanomaterials for flexible electronics	Various	Partial	X	✓	Partial	(3)
2025	Polymer-coated metal/metal oxide nanoparticles	Various	Partial	X	✓	✓	(4)
2017	Microfluidized graphene ink	Inkjet / Printed electronics	✓	X	✓	Partial	(5)
2019	Inkjet-printed graphene conductive patterns	Inkjet printing	✓	X	✓	Partial	(6)
2026	2D graphene-based electronic systems	Various	Partial	X	✓	Partial	(7)
2022	Carbon paste systems (morphology vs performance)	Screen printing	X	X	✓	✓	(8)

2025	Water-based carbon black ink	Screen printing	✓	Partial	✓	Partial	(9)
2025	CNT / Corn-Starch / PVA (Present Work)	DIW	✓	✓	✓	✓	Current study

## Materials and Methods

### Materials

Multi-walled carbon nanotubes (purified >95 percent) were acquired from Techinstro India. The specific surface area of the CNTs used in the experiment was only approximated as  $\sim 200 \text{ m}^2 \cdot \text{g}^{-1}$ , as shown in the technical datasheet supplied by the supplier, with an average outer diameter of 10-20 nm and a length of 5 to 15  $\mu\text{m}$ . These geometrical parameters were chosen because they could provide effective percolation network formation at moderate loading levels. The cornstarch (analytical grade) purchased at RK World Infocom Pvt. Ltd. was used as a biodegradable polymeric matrix component. Polyvinyl alcohol (PVA, degree of polymerization 1700-1800, 98-99% hydrolysed) was provided by Bansa India Corporation and was used as a secondary binding agent to increase the film-forming properties and mechanical strength (12).

A co-solvent called ethylene glycol (EG,  $\geq 99\%$  purity, purchased from Akshar Exim Co. Pvt. Ltd.) was used to control rheological behavior and drying properties (13). Triton X-100 (non-ionic surfactant, analytical grade) was introduced at constant concentration to ensure that the CNT dispersed by lowering surface tension and minimizing agglomeration of the nanotube (14). All materials were tracked by batch number to enable the experiment to be repeated as well as traced. The choice of materials included the necessity to balance between electrical conductivity, printability and environmental sustainability. The key conductive phase was done using CNTs and the binder functionality was done using starch and PVA, as they are eco-compatible fractions.

**Table 2:** Composition of Formulated Conductive Ink Samples (wt %)

Sample No	CNT (wt %)	Corn Starch (wt %)	PVA (wt %)	Ethylene Glycol (wt %)	Triton X-100 (wt %)
1	5	10	20	60	5
2	5	15	20	55	5
3	5	20	20	50	5
4	10	10	15	60	5
5	10	15	15	55	5
6	10	20	15	50	5
7	15	10	10	60	5
8	15	15	10	55	5
9	15	20	10	50	5

A total of nine conductive ink formulations were developed by adjusting the CNT (5-15 wt %) concentration, corn starch (10-20 wt %) concentration and PVA (10-20 wt %) concentration without affecting the EG and Triton X-100 concentrations as shown in Table 2. Triton X-100 concentration was set at 5 wt %, which was determined during initial dispersion experiments, with lower concentrations below 3 wt % leading to

visible agglomeration and higher concentrations above 5 wt % leading to excessive foaming and likely interference with conductive pathways. The chosen concentration is thus a compromise that is a balance between the dispersion stability and the continuity of the electrical networks, which is compatible with the surfactant-assisted CNT dispersion already reported in previous studied (15, 16).

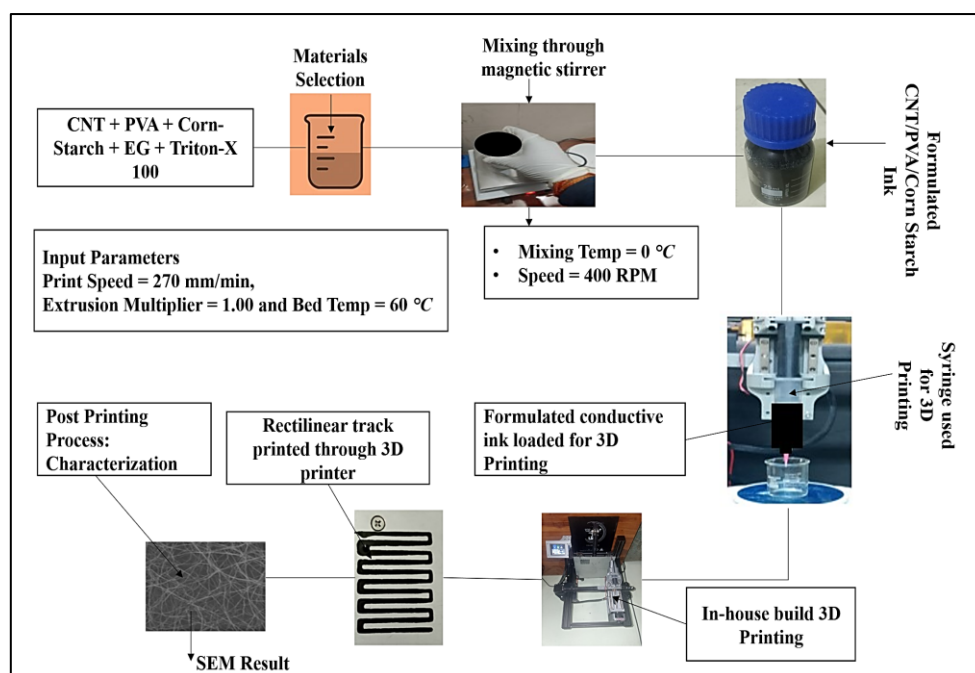


**Figure 1:** Ink Formulation and Processing Workflow

To prepare the CNTs, magnetic stirring of the suspension at 400 rpm was performed for 30 minutes in the presence of Triton X-100 at ethylene glycol concentration, as shown in Figure 1. Ultrasonication was then achieved by application of a probe sonicator set at 40 kHz and having a power output of 200 W (60% amplitude). The duration of sonication was 20 min and the dispersion lasted under controlled temperature conditions and in this case, the dispersion vessel was submerged in an ice-water bath to ensure that the temperature did not exceed 30°C. This measure helped to avoid thermal degradation of polymer elements and reduce viscosity drift due to local heating (17).

After the dispersion of CNT, the addition of cornstarch and PVA was done progressively under continuous stirring to establish even homogenization. The overall time that the ink required to mature before printing was 24 hours under ambient lab conditions ( $25 \pm 2$  °C), during which the polymer was fully hydrated, the viscosity stabilized and the air bubbles had to be released (18, 19). This intermediate maturation stage led to rheological uniformity and repeatable extrusion behavior when doing DIW processing. The prepared inks were kept in airtight vessels to avoid the evaporation of the solvents and change of viscosity before usage.

## Methods

A Taguchi Design of Experiment (DOE) was used to optimize the ink composition using fewer experimental runs. The selection of an L9 orthogonal array ( $3^3$  design) was made, including 3 independent control factors (CNT content, Cornstarch content and PVA content), to be assessed in three levels. The performance responses were viscosity, electrical conductivity and print fidelity (20). Signal-to-noise (S/N) ratios were calculated by using: Larger-is-better criterion for viscosity (to ensure DIW-compatible rheology). The response ranking and main effect plots were created through Minitab Statistical Software (Version 21). This statistical methodology facilitated the identification of the most robust formulation with balanced electrical and rheological performance, thereby enhancing the reproducibility and quality of the optimization process (21).

The ink became optimized and the quantity was loaded into airtight syringe barrels with a 0.8 mm nozzle. A DIW based manufacturing system was used at 0.4 MPa extrusion pressure,  $270 \text{ mm} \cdot \text{min}^{-1}$  print velocity and at 0.4 mm layer height to create printing was carried out. These parameters were chosen through initial extrusion experiments in order to have constant filament deposition and dimensional faithfulness (22, 23). To determine structural stability and conductive performance in printed samples, printed samples were dried under ambient conditions. The incorporation of EG

controlled solvent evaporation and, hence, minimized cracking caused by the shrinkage and enhanced the interlayers adhesion. Although EG slightly increased the drying time relative to aqueous only system, it increased the rate of conductive network forming by reducing capillary-based re-agglomeration of CNTs (24).

The rheological behaviour in this case was measured by means of a rotational viscometer (Model: LMDV 200, LABMAN). Measurements were done using spindle LV-3 within a range of 0.1-100  $s^{-1}$  at  $25 \pm 1$  °C. This range was chosen to approximate shear conditions that are observed in DIW extrusion (25). The inks exhibited shear-thinning behaviour, which is an essential requirement of DIW, where viscosity drops as a result of shear stress applied to the ink and returns to shape once deposited to keep shape fidelity (26, 27).

A four-point probe method was used to measure electrical conductivity as a way of avoiding the error of contact resistance that is often present in

two-point measurements. The methodology made sure that intrinsic conductivity of the printed films was accurately determined (28, 29). The thermal stability was measured through Thermogravimetric Analysis (TGA) at 25 °C to 800 °C at heating rate of 10 °C·min<sup>-1</sup> in the presence of nitrogen. The temperatures of onset degradation ( $T_{5\%}$  and  $T_{10\%}$ ) were picked and their percentages of residual mass were quantitatively compared (30, 31). Transform Infrared Spectroscopy (FTIR) was used to perform structural and morphological characterization, where chemical interaction was analysed, X-ray Diffraction (XRD) to characterize crystallinity and Scanning Electron Microscopy (SEM) to characterize CNT dispersion and the formation of percolation networks (32, 33).

## Results and Discussion

The behavior of shear viscosity vs shear rate for each of the nine produced conductive ink samples is displayed in Figure 2.

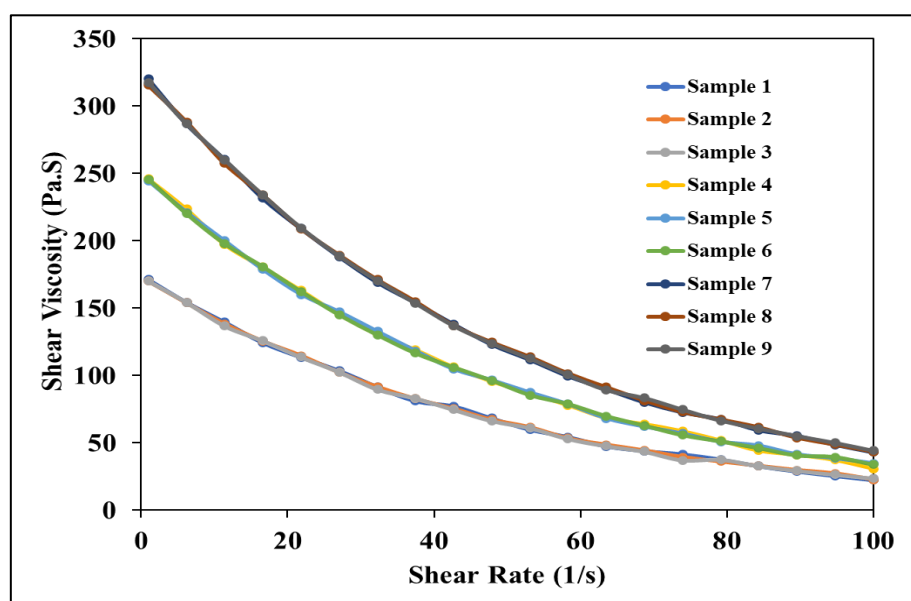


**Figure 2:** Shear Viscosity vs Shear Rate for Formulated Conductive Ink

The data follow distinctly a shear-thinning pattern, which is typical of pseudoplastic non-Newtonian fluids (34). On low shear rate, viscosity is relatively elevated owing to entrapment between CNTs, starch chains and PVA chains resulting in a percolative micro-network that is resistant to flow. This network increasingly becomes aligned with the flow direction as shear rate increases decreasing internal friction and, by extension, viscosity. At higher CNT contents (Samples 7-9)

the viscosity is much higher because the inter-particle interaction and van der Waals forces between individual CNT bundles are increased (35, 36). This type of rheological behavior is favourable to DIW as the behavior encourages the control of extrusion stability as well as the prevention of ink spreading following deposition (37).

The FTIR spectra of the nine conductive ink samples that were generated are shown in Figure 3. The samples show characteristic absorption

bands that correspond to their chemical components. The general plateau at  $3300\text{ cm}^{-1}$  is the O-H vibrations of both PVA and starch, which are a confirmation of the presence of hydrogen bonds between the polymeric chains (38). Peaks at approximately  $2900\text{ cm}^{-1}$  are C-H stretching, at approximately  $\sim 1720\text{ cm}^{-1}$  and  $1080\text{ cm}^{-1}$  C=O and C-O starch and ethylene glycol. This slow broadening of the peaks and changes in intensities

with increasing CNT content indicate that more molecular interactions and interfaces occur in between CNTs and polymeric matrices (39, 40). This adds up to the homogenous distribution of the ink components and chemical compatibility, which is a key to enhanced electrical conduction and mechanical integrity of the end results in DIW-printed structures (41, 42).

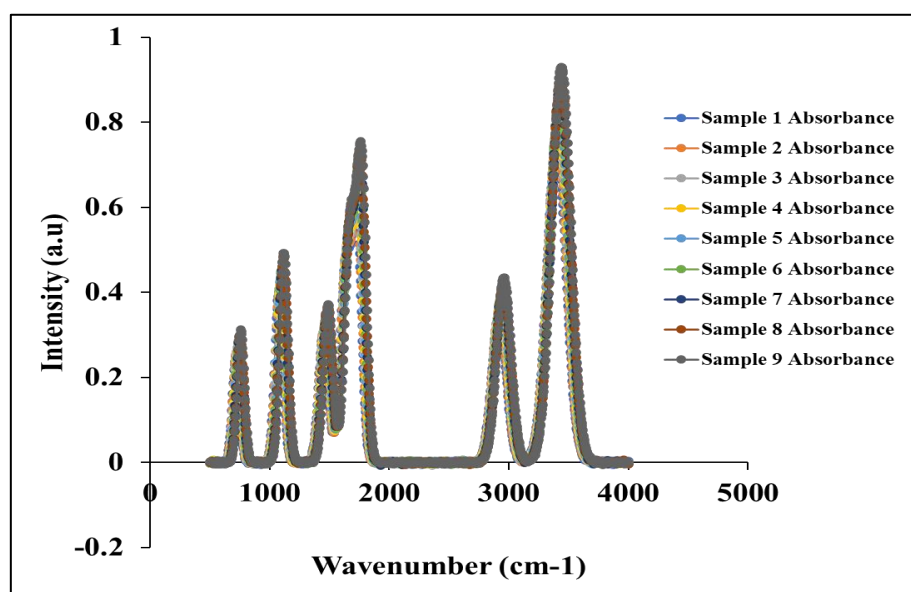


**Figure 3:** FTIR Spectra for Formulated Conductive Ink

The rheological and chemical characterization of the invented CNT, corn starch, PVA, based conductive inks establish that they exhibit an appropriate flow stability, shear-thinning rheology and interfaces with DIW printing. Viscosity range guarantees that it is easy to extrude without clogging the nozzle whereas FTIR results confirm that polymer filler networks are formed essential in charge transportation pathways (43). A combination of these results supports the optimized printability and performance of the ink providing a sound base upon which additional Taguchi-based optimization and correlation of microstructures in the future sections. The viscosity of the CNT solution increases with the CNT concentration between 5 wt % and 15 wt %, which is  $48.2\text{ Pa}\cdot\text{s}$  as to  $86.9\text{ Pa}\cdot\text{s}$ . FTIR analysis of increased filler-polymer interactions, increase in entanglement density and limited mobility of the molecules in the matrix. The high viscosity Samples 7-9 have is expected to enhance shape retention in the extrusion of DIW and underscores

the applicability of the inks to high-fidelity printed geometries in moderate shear forces. Three distinct level of the four primary control factors (CNT, corn starch, PVA and ethylene glycol) are assigned to the experimental area in Table 3, together with a constant level of Triton X-100 kept at 5 weight percent. This choice places the Taguchi L9 study in context and is indicative of a conscious effort to tie chemistry to processability, CNT levels (5-15 wt %) sample the dilute to percolative regime, corn starch and PVA levels (10-20 wt %) sample the binder-entanglement regime and ethylene glycol (50-60 wt %) sample the continuous-phase mobility and effective solids fraction (44, 45). Consequently, these transition levels span the fluid/network rheology change in low CNT/low solids compositions Favor low viscosity and facilitate extrusion and the filler-polymer an is linkages of high CNT/high binder compositions Favor high-viscosity hardened high-hydrogen bond matrices.

**Table 3:** Setting Level of Control Factors

Factor	Level 1	Level 2	Level 3
CNT (wt %)	5	10	15
Corn Starch (wt %)	10	15	20
PVA (wt %)	10	15	20
Ethylene Glycol (wt %)	50	55	60
Triton X-100 (wt %)	5	5	5 (kept constant)

By fixing Triton at 5 wt % the design isolates dispersant effects from compositional drivers, enabling clearer attribution of observed rheological responses to the main formulation factors. In practical terms, Table 2 therefore establishes a balanced and process-relevant factor space that links material chemistry to DIW constraints (extrusion pressure, filament stability and post-deposition recovery).

The nine orthogonally organized experimental runs and their measured response maximum low-shear viscosity at 25 °C are shown in Table 4, which also illustrates how the four parameters' systematic change affects bulk rheology. The measured viscosities increase progressively across the array: runs with low CNT (Samples 1-3) show

the lowest values (~48-57 Pa·s), whereas runs with high CNT and elevated starch (Samples 7-9) produce the highest viscosities (~79-87 Pa·s). This pattern is consistent with formation and densification of a percolated CNT network embedded in a viscous starch-PVA matrix: CNTs amplify hydrodynamic hindrance and inter-particle friction while starch increases continuous-phase viscosity through chain entanglement and hydrogen bonding with PVA. Ethylene glycol acts conversely as a plasticizer higher EG fractions reduce solids packing and lower measured viscosity so samples where EG is at its lower level (50 wt %) tend to show higher viscosity for comparable CNT/starch contents.

**Table 4:** L9 Orthogonal Array Design

Sample No	CNT (wt %)	Corn Starch (wt %)	PVA (wt %)	Ethylene Glycol (wt %)	Triton X-100 (wt %)	Maximum Viscosity (Pa·s)
1	5	10	10	50	5	48.2
2	5	15	15	55	5	52.6
3	5	20	20	60	5	57.4
4	10	10	15	60	5	63.1
5	10	15	20	50	5	69.5
6	10	20	10	55	5	72.3
7	15	10	20	55	5	78.8
8	15	15	10	60	5	81.6
9	15	20	15	50	5	86.9

The measured data in Table 4 thus quantify the competing roles of filler loading (dominant), binder content (significant) and solvent/plasticizer (moderating) on DIW- relevant rheology; these outcomes also indicate the practical trade-offs for DIW: higher viscosity enhances shape retention and filament stability but may demand greater extrusion pressure and influence nozzle lifetime. The Detailed S/N Ratio table shown in Table 5 is a summary of the Taguchi analysis with a larger-the-better S/N statistic used on maximum viscosity

and includes a succinct, statistically enlightened ranking of factor importance. The S/N row of CNT changes significantly between Level-1 and Level-3 (52.73 to 82.43) with a resultant  $\Delta$  (29.70) being the largest and a decisive rank of 1; this means that, the CNT concentration is the main determinant of the maximum viscosity in the studied space and the discovery agrees with the physical process of forming a network and enhancing inter-particle interactions (46)

**Table 5:** Detailed SN Ratio of Formulated Conductive Ink

Level	CNT (wt %)	Corn-Starch (wt %)	PVA (wt %)	Ethylene Glycol (wt %)	Triton X-100 (wt %)
1	52.73	63.37	67.37	68.20	67.82
2	68.30	67.90	67.53	67.90	-
3	82.43	72.20	68.57	67.37	-
Delta	29.70	8.83	1.20	0.83	0.00
Rank	1	2	3	4	5

The second most significant factor ( $\Delta = 8.83$ ) is the corn-starch factor, which validates that an increase in the content of binder causes the viscosity of the matrix to increase due to an entanglement of chains and reinforcement by hydrogen bonds, therefore, the macroscopic resistance to flow intensified. The  $\delta$  values of PVA and ethylene glycol are relatively low (1.20 and 0.83 respectively), which reflects the secondary tuning role of these factors in the chosen levels: the former is quite a minor effect of the former on the film-forming and

viscoelasticity, whereas the latter is a major influence of the former on the mobility and dilution ability. Constant Triton X-100 does not add any variance on this analysis (differences = 0). The S/N Ratio analysis in above Table 5 underpin the idea of optimization of the formulations by using CNT and starch as the main leverages to achieve target rheological windows with DIW, whereas PVA and EG are used to correct the printability and the post-print mechanics.

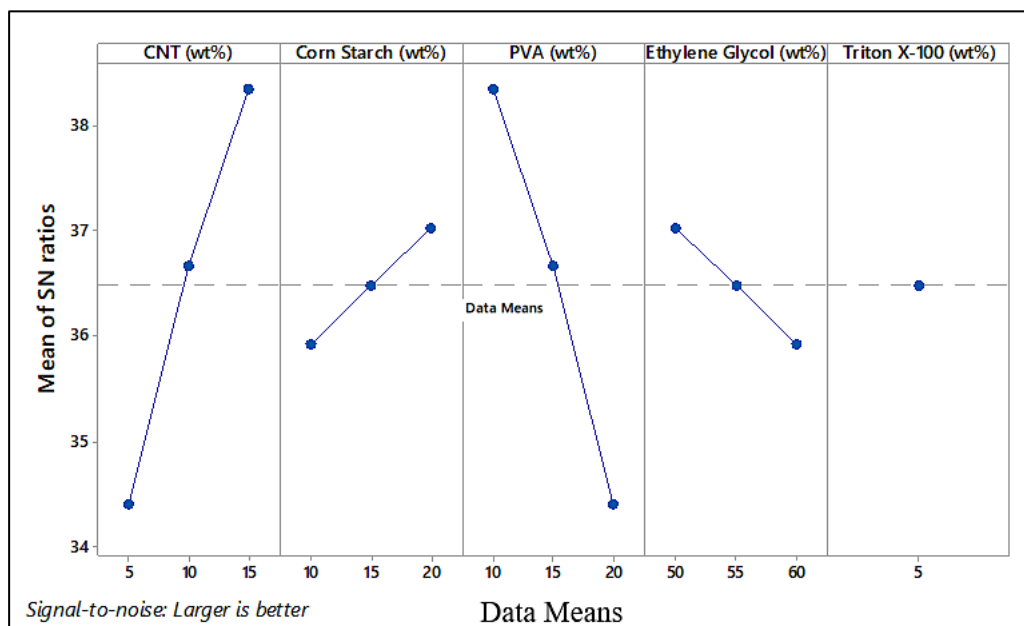


**Figure 4:** Main Effects Plot of S/N Ratio

The effect of each control factor on the average viscosity of the conductive ink formulation is shown in Figure 4. The sharp inclination of CNT implies its prevailing effect whereby high CNT content (5-15 wt %) contributes largely to the viscosity because of the intense filler-polymer affinity and filler-percolation network. Corn starch has also positive tendency, which is involved in thickening due to the formation of hydrogen bond

with PVA and CNT. Conversely, the effect of PVA is minimal, whereas ethylene glycol has a moderate tendency to decrease viscosity because it is a plasticizer. Triton X-100 is a constant, not changing. Additionally, CNT and starch are the main factors that regulate the rheology, providing appropriate viscosity to 3D print stable and precise DIW.

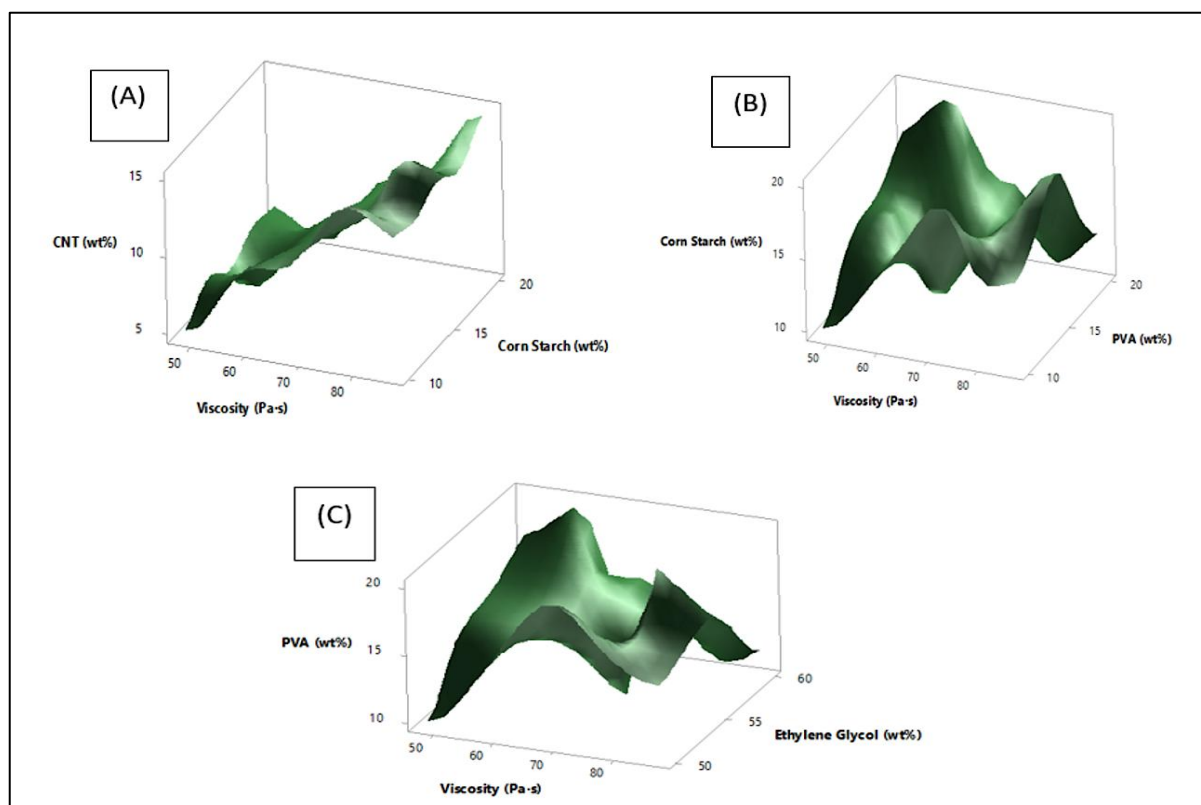


**Figure 5:** Response Surface Plots Showing Interaction Effects of Control Factors on Viscosity (Pa·s)- (A) Surface Plot of CNT (wt %) vs Corn Starch (wt %), Viscosity (Pa·s ), (B) Surface Plot of Corn Starch (wt %) vs PVA (wt %), Viscosity (Pa·s ) and (C) Surface Plot of PVA (wt %) vs Ethylene Glycol (wt %), Viscosity (Pa·s )

The interaction effects of ethylene glycol, PVA, corn starch and carbon nanotubes on the 3D response surface and their impact on the viscosity of the resulting conductive ink are depicted in Figure 5. Figure 5(A) shows that viscosity rises considerably with both CNT and corn starch, which points to the fact that fillers have strong interactions with the binder to augment the creation of a network and shear strength. Figure 5(B) indicates that the viscosity increases moderately as the levels of both starch and PVA increase because of the hydrogen bonding and entangling polymers. Viscosity versus ethylene glycol is slightly decreasing in Figure 5(C), which proves that it is a plasticizer lowering friction inside the compound. In general, CNT and starch can be considered to have dominating synergistic behavior, which guarantees the rheological stability needed to obtain a uniform deposition of the layer when using DIW in 3D printing.

The Taguchi L9 analysis, which is described in the chosen design space, showed quite clearly that CNT loading is the most significant factor that has its impact on low-shear viscosity and then corn

starch, with relatively low effects of PVA and ethylene glycol. The ranking suggests that increased CNT and starch content are synergistic in the influence on increased viscosity due to better network formation and polymeric entanglement, which retain filament shape during extrusion. The Taguchi method therefore offered an efficient statistical method of establishing the key drivers in a lower number of experiments, resulting in an optimal level of formulation an ideal condition of high CNT, high starch, moderate PVA and low EG to provide the required rheological performance to be used in DIW applications.

The practical benefit of such optimization is that it directs the work of formulation toward the most meaningful parameters, with which a lot of trial and error can be avoided. The Taguchi results presented as quantified values of  $\Delta$  enable the research to allocate resources to CNT and starch tuning with PVA and EG being regarded as secondary modifiers. Sample 9 (15 wt % CNT, 20 wt % starch, 15 wt % PVA, 50 wt % EG, 5 wt % Triton X-100) showed the greatest calculated viscosity of 86.9 Pa·s . This state was found by

Taguchi analysis (A3B3C3D1) as the optimum rheological choice amongst equal performance. The achieved viscosity is in the commonly reported values of Direct Ink Writing of polymer-carbon composite systems where the printable inks exhibit viscosities of roughly  $\sim 10$  and  $10^2$  Pa·s at low shear rates, depending on the diameter of the nozzle and the extrusion pressure.

Specifically, CNT-based DIW recipes often demand viscosities between 50-100 Pa·s to be sufficiently high to retain shape after extrusion and still allow flow of filaments continuously. A viscosity outside on either side of this range can lead to filament spreading and loss of dimensional fidelity, but overly high viscosity can cause unstable extrusion and high levels of pneumatic pressures. Thus, the operationalized measurement of 86.9 Pa·s is a good compromise between both shear-thinning flow during extrusion and rapid structural recovery after deposition. According to this rheological analysis, the DIW validation of Sample 9 was carried out to make sure both processability and geometric stability were ensured when 3D printing.

A step towards Taguchi optimization to DIW printing would include organized rheological verification, slight compositional adjustment and a test run printing verification. Initial printing should be undertaken with a nozzle dimension of 0.8 mm, extrusion multiplier 1.00, printing speed 270 mm/min and bed temp. 60 °C to print basic geometries measuring the accuracy of dimensions and solids filament viability. After 3D printing process characterisation such as SEM, XRD, TGA and Electrical Conductivity will be done systematically. The Sample 9 may be considered as the most viable initial formulation and any final optimization may be informed using specific Taguchi knowledge, which will allow the close-out optimization of formulation to be evidenced-based and ultimately generate functional 3D-printed components.

Taguchi-optimized CNT corn starch/PVA conductive ink, rheologically and microstructurally characterized, was used in Direct Ink Writing (DIW)-based 3D printing experiments, as shown in Figure 6. Printing experiments were carried out using a DIW 3D

printer which was customized and fitted with a Flexible Accurate Extrusion system as in Figure 6(A). The ink was found to display a steady shear-thinning behavior, viscous behavior of high rank ( $\approx 86.9$  Pa·s) and even distribution of CNTs, established by SEM and FTIR. The properties guaranteed continuous extrusion, retention of shape and a constant stacking of layers as the printing was taking place.

A 30 mL syringe barrel with a blunt-tipped nozzle was charged with the optimized ink before printing. According to the rheological profile, the extrusion multiplier 0.75 was chosen to be low to ensure even deposition of filament without any clogging of the nozzle. A printing speed 270 mm/s and temp 60 °C was also set to ensure a smooth deposition of the filament. This printing trials were made at ambient temperature and capitalized on favourable viscoelastic behaviour of the formulation. Several test geometries were created in order to test the printability. The uniformity of the flows and the width of the filaments was initially studied by extrusion of a straight-line path as shown in Figure 6(B-C). Extruded filament consisted of uniform thickness and minimal spreading out of lateral effects, balanced viscosity and surface tension were ensured. An excellent lateral adhesion and continuous extrusion around and through sharp turns with a rectilinear structure printed subsequently, as shown in Figure 6(D) showed better binder-CNT network stability.

Moreover, the circular disc specimens were printed and were used to evaluate robustness in both single and multi-layer deposition. A single-layered disc as shown in Figure 6(E) was taken with a uniform surface texture and loss of edges was minimal. A double layer disc, depicted in Figure 6(F) resulted in better dimensional integrity, which assured the presence of good interlayer bonding. Figure 6(G) depicts that the multi-layer solid disc displayed high density, compact stacking in the absence of delamination and internal porosity, which confirmed the structural integrity of the optimized ink and its extrusion fidelity.

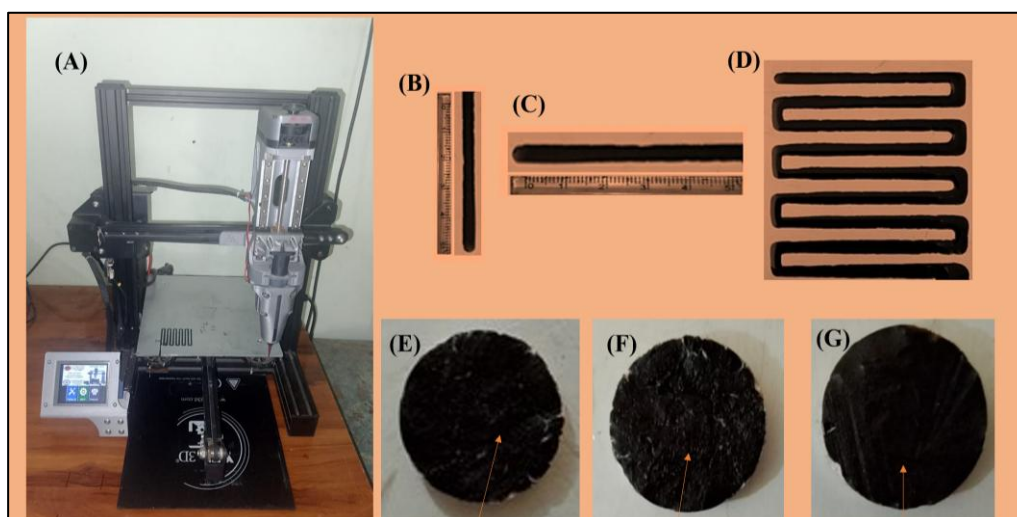


**Figure 6:** DIW Printing Setup and Printed Structures of Optimized CNT-Corn Starch/PVA Ink - (A) DIW Printing Setup, (B) Single-line Extrusion, (C) Straight Printed Track, (D) Rectilinear Pattern, (E) Single-layer Disc, (F) Double-layer Disc and (G) Multi-layer Disc

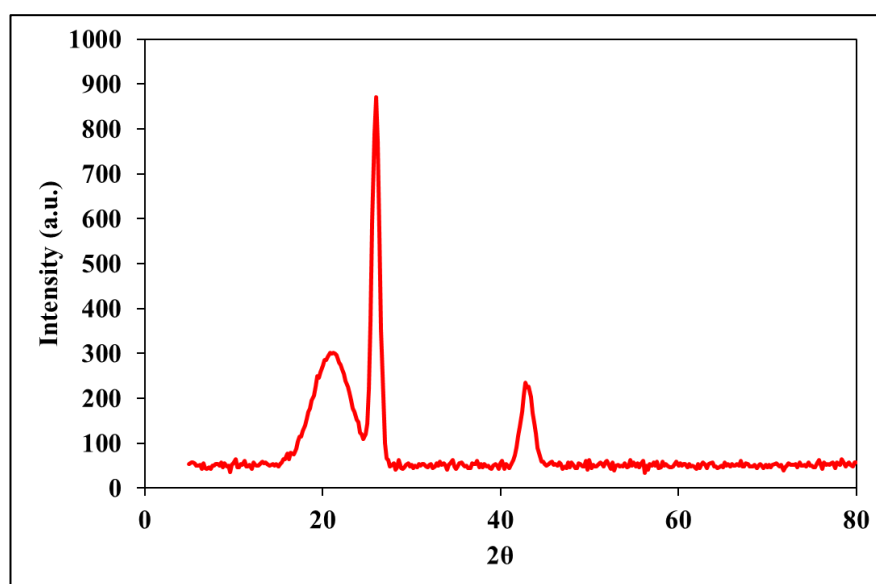


**Figure 7:** XRD Pattern of Printed Composite Ink

A broad amorphous halo at centers of  $20\text{-}22^\circ 2\theta$  and a sharp, noticeable feature at  $\approx 26^\circ 2\theta$  with a smaller feature at  $\approx 43^\circ 2\theta$  are the two main aspects of the X-ray diffraction pattern depicted in Figure 7. The wide halo is used to indicate the semi-crystalline structure of the polymeric matrix of corn-starch and PVA and implies low-order levels over a long-range post-dispersion and printing of CNTs. The steep peak at  $\approx 26^\circ 2\theta$  angle represents the graphitic structure of multi-walled carbon nanotubes and this shows that the CNT graphitic structure remains intact during the formulation and DIW treatment. The less intense and reduced width of the  $26^\circ$  peak suggests some local alignment or stacking of the CNTs in printed filaments, which enables flow of the electricity. A

high level of CNT polymer interfacial interaction and shear during extrusion enable filler alignment at the expense of increased amorphous of the polymer mass (26).

The thermogravimetric analysis shown in Figure 8 showed that the CNT-starch-PVA composite ink has a typical multi-stage degradation behaviour. The early slight weight loss of less than  $120^\circ\text{C}$  can be attributed to the evaporation of the absorbed water and the remaining solvent. Thermal degradation severe thermal degradation, based on  $T_5\%$  and  $T_{10}\%$  criteria was found to begin at about  $185^\circ\text{C}$  and  $230^\circ\text{C}$  respectively. These values demonstrate that it is thermally stable enough to be used in printed electronic and sensing applications at low temperatures.

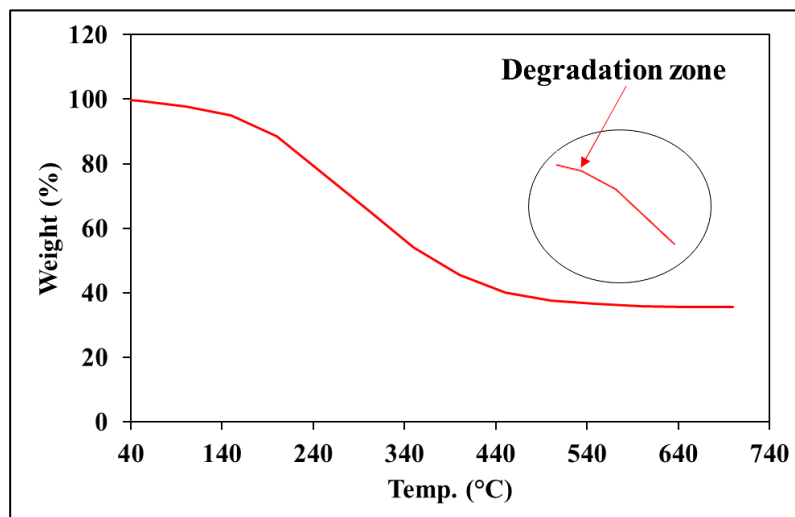


**Figure 8:** TGA Thermogram of Printed Composite Ink

The main process of decomposition was carried out between 250 and 400°C, which is explained by the deterioration of starch and PVA polymer backbones. The rate of degradation was slowed below 400°C and the result was a stable residue of carbonaceous products. Mass content at 800°C was between 18 and 28%, with an increment depending on CNT loading. This increase in char confirms that the CNT network is thermally stable and reinforcing, which inhibits the volatilization of polymers and enhances the retention of carbonaceous structures. Three advantages of the CNTs are the improved electrical performance of the composite system in printing and thermal strength (34).

The enhanced conductive ink's microstructural performance and subsequent printing capacity (SEM characterization) are both improved in Figure 9. The CNT bundles are only partially disentangled and polymer is uniformly encapsulated as demonstrated in Figure 9(A-C). The corn-starch/PVA binder matrix creates a continuous and smooth film which attaches itself firmly to individual CNTs, decreasing agglomeration and enhancing dispersion homogeneity. The academic rationale behind this polymer coating is critical due to materials science

since it is used to reduce interfacial tension, increase the wetting of CNT and stabilize the ink to be sheared. The smaller surface morphology of the micrographs is associated with optimized rheological profile ( $\approx 86.9$  Pa·s), which guarantees the absence of defects during extrusion and maintenance of shape in DIW.

Further microstructural optimization is shown in Figure 9(D-F) with the CNTs being a dense and interconnected network of percolation. The CNT web comes out as cross-linked through strong van der Waals attraction and physical entanglement forming consecutive electron pathways crucial in conductivity (25, 26). According to the standardized distribution of CNT throughout the binder matrix, it can be stated that there is good dispersion, supported by Triton X-100 and ethylene glycol which do not allow phase separation and improves flow characteristics. The fact that it has no void, cracks or discontinuities, verifies that the Taguchi optimized formulation has microstructural stability that is sufficient to print multi-layers. Its ability to generate dependable flexible electronic component explains the continuity of the percolation network that increases the electrical response and structural fidelity of the ink.

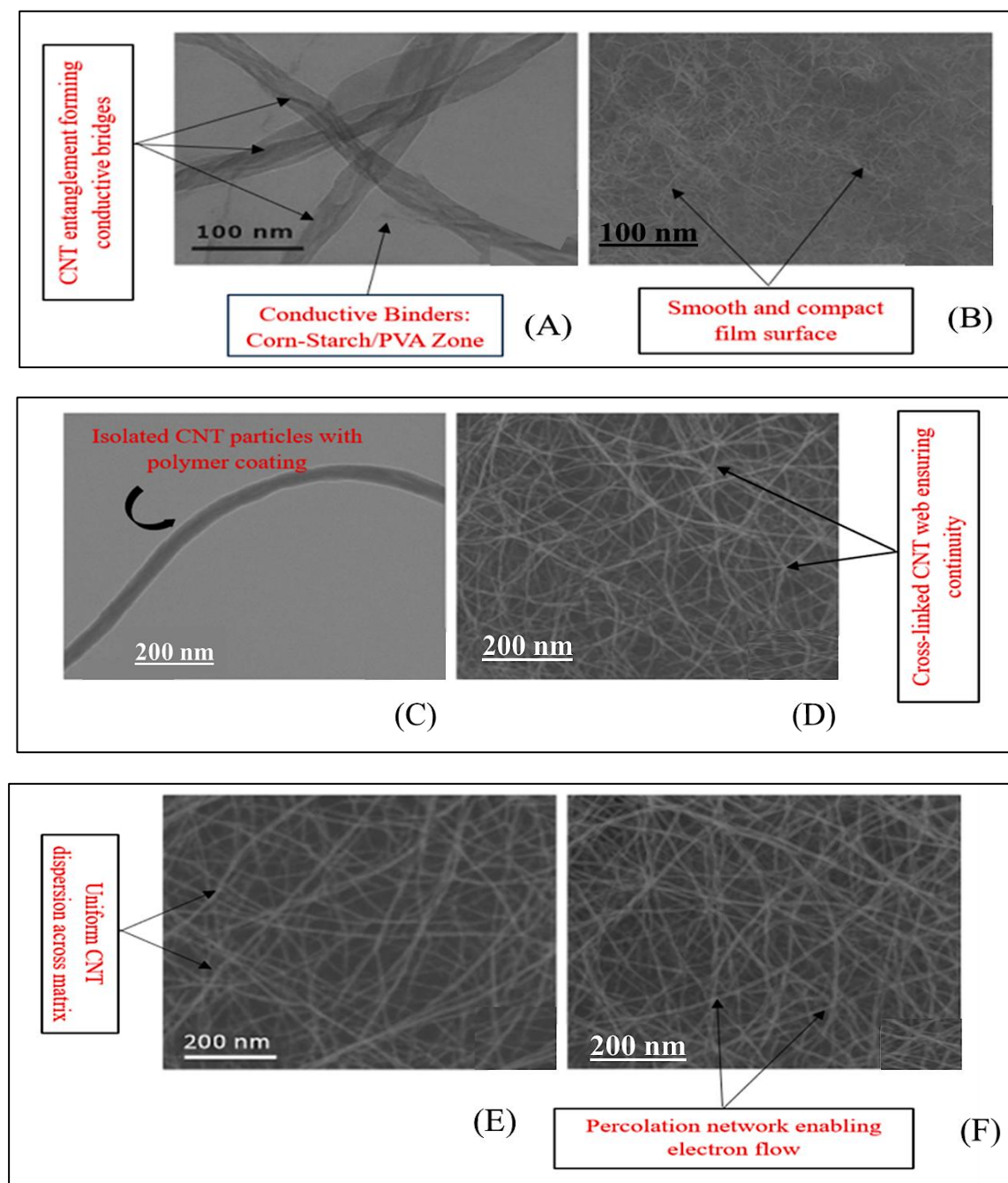


**Figure 9:** SEM Micrographs of Printed Composite Ink, (A) High-resolution View Showing Individual CNT Bundles (Scale Bar 100 nm); (B) Low-magnification Network Overview; (C) Curved CNT Strand (Scale Bar 200 nm); (D-F) Progressively Larger-area Topographies of the Printed Filament Surface (200 nm Scale)

The rheological, structural and thermal properties of the ink had a positive correlation with the printing results of the DIW method. Homogeneous CNT dispersion seen in SEM, semi-crystalline structure of polymer measured by XRD and increased thermal stability seen through TGA all allowed the extrusion to be stable and the layer better adhesive to the printing process. These SEM analyses indicate that the optimized ink is quite suitable as an eco-friendly conductive ink for 3D

printing due to the use of flexible electronics, low-cost sensors and biodegradable circuit components.

When CNT loading is loaded from 5 to 15 wt %, Figure 10 illustrates significant improvement in bulk electrical conductivity. The evolution of conductivity indicates classical percolation behaviour of conductive polymer composites. The conductive pathways at 5 wt % CNT are partially isolated and therefore, there is limited electron

transport, which consists of tunnelling resistance (47). There is a very steep gradient between 5 and 10 wt % which is an indication that the system has passed the threshold of electrical percolation and it has created a continuous interconnected network of CNT. Not only up to this point, but also

beyond, the degree to which inter-tube contact density is improved by increasing the wt % higher, to 15 wt %, is sensitised tunnelling distances and, therefore, the charge carrier mobility is augmented.

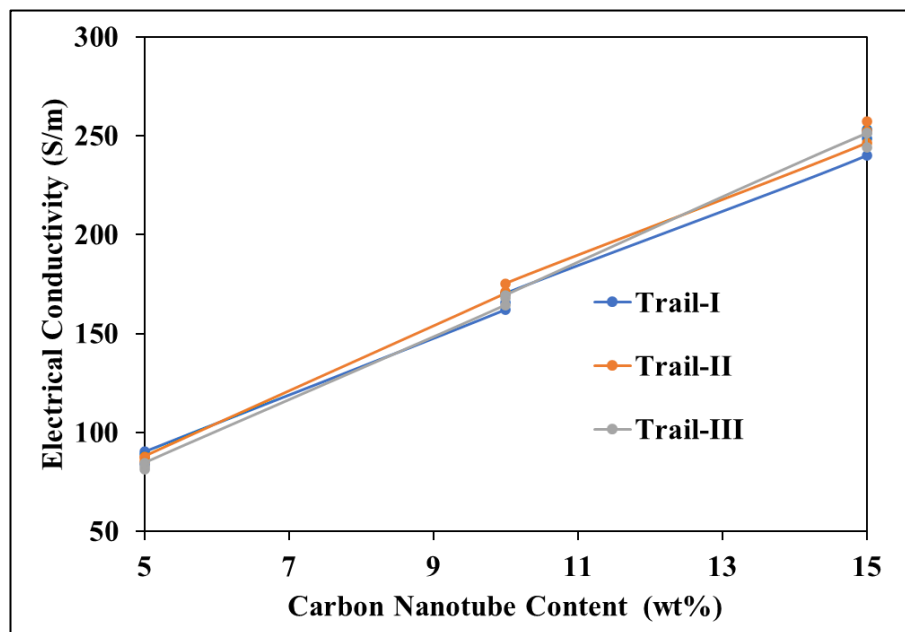


**Figure 10:** Electrical conductivity vs Carbon Nanotube Content

Optimal formulation of 15 wt % was found to have conductivity between  $10^{-1}$  and  $10^0$   $S \cdot cm^{-1}$ . The given ink shows better electrical performance in a biodegradable matrix when compared with the reported system of starch-based carbon inks ( $10^{-3}$ - $10^{-2}$   $S \cdot cm^{-1}$ ) and commonly used Polymer systems with CNTs ( $10^{-2}$ - $10^{-1}$   $S \cdot cm^{-1}$ ). Even though commercial graphite-based inks can go as

high as  $10^0$ - $10^1$   $S \cdot cm^{-1}$ , they often use non-environmentally friendly binders (48). These electrical conductivity analysis outcomes support the ruling of CNT content as a determinant of functional performance, in addition to the fact that the DIW trade-off inevitably entails increased conductivity versus greater viscosity, which is necessary to support extrusion stability.

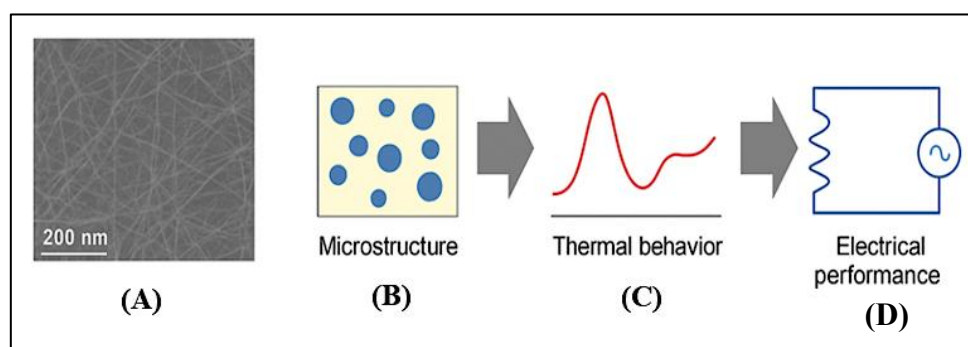


**Figure 11:** Correlation of Characterization Results of CNT-Corn Starch/PVA Conductive Ink

The results of the optimisation process of the deposit, printability evaluation and the characterisation of the material used to produce CNT/Corn Starch/PVA conductive ink system, as discussed in Figure 11, represent a concerted confirmation of the CNT/Corn Starch/PVA

conductive ink system after 3D printing. Confirmation of the DOE results confirmed that CNT loading was the strongest factor when it came to electrical conductivity, viscosity and extrusion behavior. Optimized range was used to facilitate percolation network formation without interfering

with the flowability or dimensional fidelity when printing. This compatibility was confirmed in the course of the printability experiment, in which the rheology-optimized compositions exhibited the benefit of easy extrusion, consistent filament geometry and defect-free printability- a sign that the rheology-electrical functionality balance is achieved.

In this regard, SEM analyses of Figure 11(A) show the micrographs of mixed composition indicate a continuous and interlaced network of CNTs within the polymer matrix that effectively triggers dispersion and high filler-matrix interfacial forces (25, 26). This microstructure shows a direct correlation between the measured trend of conductivity with the CNT loading, where the rate of electrical performance rose steadily with CNT loading and corresponded with classical percolation theory. XRD results presented in Figure 11(B) indicate the characteristic semi-crystalline markers of both starch and PVA and clear CNT peaks, which confirmed that the material crystallinity of the polymer did not decrease as CNTs were incorporated successfully (26).

Figure 11 (C) thermal analysis showed a slower degradation of CNT reinforced samples indicative of increased thermal stability to undergo DIW processing and post-curing cycles (34). The combination of these results confirms that the formulation is optimized to fit the processing and performance requirements; that is, the behavior of materials in extrusion and curing is controlled. Further correlations as shown in Figure 11 (D) reinforce the relationship between the material structure as well as the outcome of electrical properties (43). It also provides a schematic correlation to explain the relationship between the microstructure and the ability of the material to heat and the electrical output produced by the system, indicating that CNT networking and the ordering of polymer matrixes complement each other in terms of conductivity and material stability (47, 48).

The shear-thinning rheology coupled with moderate thermal stability and percolation electrical conductivity place the developed ink in different flexible electronic applications (40, 41). Specifically: (a) Strain sensors: CNT percolation network CNT percolation network allows piezoresistive behavior, i.e., change in resistance under mechanical deformation can be utilized in

wearable strain monitoring, (b) Flexible interconnects: Signal transmission in low-power signal architectures requires conductivity of the  $10^{-1}$ - $10^0$  S-cm<sup>-1</sup> range and (c) Printed heaters: Joule heating performance: Because the conductive pathways are stable and the heating system is thermally resistant, up to approximately ~180 °C operating temperatures.

Furthermore, the biodegradable starch-PVA matrix implies that the system can be used in other applications that involve biodegradability (disposable biosensors and transient electronics) and in which minimizing the environmental impact is essential. The rheological suitability with DIW also allows one to fabricate bespoke sensor geometries and tracks, micro-patterns, multilayer, etc. Therefore, in addition to laboratory level formulation, the fabricated ink has a promising future in printed electronic systems that are sustainable.

## Conclusion

The research study was able to developed and optimize a CNTs/Corn-Starch/PVA-based conductive ink for DIW-based 3D printing process and the optimized ink parameters were selected through Taguchi design and multi-stage characterization. They were optimized to achieve the rheological, structural and thermal appropriateness and functionality of the composite ink in printable electronic uses. The main research outcomes are following as:

- a) Optimization CNT loading was the most significant variable in rheology and printability according to Taguchi L9 optimization.
- b) In the optimal formulation (CNT 15 wt %, Corn Starch 20 wt %, PVA 15 wt %, EG 50 wt %), viscosity was 86.90 Pa·s.
- c) Multi-layer deposition multi-layer deposition was defect-free and showed stable extrusion and linear geometries in DIW printing.
- d) XRD identified a semi-crystalline composite-based matrix with increased structural ordering of CNT.
- e) TGA showed high thermal stability up to approximately 35°C confirming better polymer-CNT contact.
- f) SEM showed uniform CNT dispersion and continuous pathways of conductive propagations in the polymer matrix.

- g) Optimized print parameters showed a strong interlayer adhesion and great geometric fidelity at the printed samples.
- h) The combined rheological, structural and thermal analysis characterisation outcomes proven the appropriateness of the ink in flexible electronics.

Despite the promising results of this research study, it has certain limitations. Only laboratory scale was evaluated on electrical conductivity, but long-term stability of electrical conductivity when subjected to the environment was not investigated. Additionally, in this research, limited part fabrication was performed. Moreover, this work could not have regarded the large-scale printing and integration with the real objects. Further studies are advised on durability measurement, mechanical-electrical coupling behavior, scalability of formulation and performance validation in real-life flexible electronic applications.

In the conclusion, this research study demonstrates that the CNT coupling of Corn Starch/PVA composite ink satisfies all the key requirements of DIW 3D printing, such as balanced viscosity, thermal stability and uniform microstructure. The use of the percolated CNT network increased conductivity and exemplified the success of the formulation design for functional printing.

### Abbreviations

°C: Degree Celsius,  $\mu\text{m}$ : Micrometer, CNT: Carbon Nanotube, DIW: Direct Ink Writing, DOE: Design of Experiments, EG: Ethylene Glycol, nm: Nanometer, PVA: Polyvinyl Alcohol, S/N: Signal-to-Noise Ratio, wt %: Weight Percentage.

### Acknowledgements

The authors are quite grateful to the Central Instrumentation Facility (CIF) of Lovely Professional University (LPU) that offered all their help to carry out all the characterization studies, such as the determination of viscosity, FTIR, TGA, XRD and SEM. CIF has played a significant role in assisting in technical analysis and the use of high-quality instruments to complete this research work successfully.

### Author Contributions

Jhunjhun Kumar Mishra: investigation, analysis, writing, Vishal Francis: software analysis,

supervision, technical critique. After debating the results and proofreading of the article, the two authors ultimately agreed to submit the finished product. We were able to establish the research's academic integrity, methodological soundness and scientific validity thanks to the test drive.

### Conflict of Interest

The authors confirmed that there is no conflict of interest in the publication of this research.

### Data Availability Statement

On the reasonable request, the corresponding author can provide the data used and justify the findings of this research work.

### Declaration of Artificial Intelligence (AI) Assistance

The authors declare no use of artificial intelligence (AI) for the write-up of the manuscript.

### Ethics approval

Not Applicable.

### Funding

No fundings for this research work.

### References

1. Smedt SD, Attaianese B, Cardinaels R. Direct ink writing of particle-based multiphase materials: From rheology to functionality. *Current Opinion in Colloid & Interface Science*. 2025;75:101889. <https://doi.org/10.1016/j.cocis.2024.101889>
2. Hong H, Jiang L, Tu H, *et al.* Formulation of UV curable nano-silver conductive ink for direct screen-printing on common fabric substrates for wearable electronic applications. *Smart Mater Struct*. 2021;30(4):045001. doi: 10.1088/1361-665X/abe4b3
3. Huang Q, Zhu Y. Printing conductive nanomaterials for flexible and stretchable electronics: A review of materials, processes and applications. *Adv Mater Technol*. 2019;4(3):1800546. <https://doi.org/10.1002/admt.201800546>
4. Atik R, Islam R, Ariza Gonzalez M, *et al.* Recent advances in polymer-coated metal and metal oxide nanoparticles: From design to promising applications. *Nanomaterials*. 2025;15(22):1744. <https://doi.org/10.3390/nano15221744>
5. Karagiannidis PG, Hill EW, Lin C-T, *et al.* Microfluidization of graphite and formulation of stable graphene inks for printed electronics. *ACS Nano*. 2017;11(3):2742–55. doi: 10.1021/acsnano.6b07735
6. Karim N, Afroj S, Tan S, *et al.* All Inkjet-printed Graphene-silver Composite Ink on textiles for Highly Conductive Wearable Electronics Applications. *Sci Rep*. 2019;9:8035. doi:10.1038/s41598-019-44420-y

7. Alaraj AM, Esmaeil AA, Khamis MA, *et al.* Pioneering advancements of 2D graphene: Energy and electronics applications. *Opt Quant Electron.* 2026;58:4.  
<https://doi.org/10.1007/s11082-025-08534-0>
8. Potts SJ, Korochkina T, Holder A, *et al.* The influence of carbon morphologies and concentrations on the rheology and electrical performance of screen-printed carbon pastes. *J Mater Sci.* 2022;57:2650–66.  
<https://doi.org/10.1007/s10853-021-06724-1>
9. Jéssica RC, Robert DC, Elena B, *et al.* Water-based conductive ink for the production of carbon black screen-printed electrodes and the detection of tryptophan. *ACS Appl Electron Mater.* 2025;7(12):5599–610.  
<https://doi.org/10.1021/acsaelm.5c00550>
10. Tran TS, Dutta NK, Choudhury NR. Graphene inks for printed flexible electronics: A review of formulation, rheology, stability and applications. *Adv Colloid Interface Sci.* 2018;261:41–61.  
doi: 10.1016/j.cis.2018.09.003
11. Ben SL, Ayadi B, Alharbi S, *et al.* Recent advances in additive manufacturing: A review of current developments and future directions. *Machines.* 2025;13(9):813.  
<https://doi.org/10.3390/machines13090813>
12. Maier AS, Lackner F, Fink J, *et al.* High-fidelity direct ink writing of poly(vinylphosphonate)-reinforced polysaccharide inks with tunable properties. *ACS Appl Poly Mater.* 2025;7(3):1752–62.  
<https://doi.org/10.1021/acsapm.4c03517>
13. Wu JT, Hsu STC, MH Tsai, *et al.* Conductive silver patterns via ethylene glycol vapor reduction of inkjet-printed silver nitrate tracks on a polyimide substrate. *Thin Solid Film.* 2009;517(21):5913–7.  
doi: 10.1016/j.tsf.2009.04.049
14. Baglioni M, Poggi G, Ciolli G, *et al.* A Triton X-100-based microemulsion for the removal of hydrophobic materials from works of art: SAXS characterization and application. *Materials.* 2018;11(7):1144.  
doi: 10.3390/ma11071144
15. Dang MC, Dang TMD, Fribourg-Blanc E. Silver nanoparticles ink synthesis for conductive patterns fabrication using inkjet printing technology. *Adv Nat Sci Nanosci Nanotech.* 2015;6(1):015003.  
doi: 10.1088/2043-6262/6/1/015003
16. Prabhakaran R, Pitchipoo P, Rajakarunakaran S, *et al.* Experimental investigation and optimization of process parameters on digital light processing (DLP) 3D printing process based on Taguchi-grey relational analysis. *Proc Inst Mecha Eng E J Pro Mech Eng.* 2024;238(4):1884–93.  
doi: 10.1177/09544089241236267
17. Zhao C, Wang J, Qian B, *et al.* Preparation of paper-based conductive pattern for 3D printing. *J Phys Commun.* 2023;7:035003.  
doi: 10.1088/2399-6528/ac060d
18. Eghan B, Ofori EA, Seidu RK, *et al.* Systematic review of conductive inks for e-textiles: Formulation, printing methods, challenges and opportunities. *AATCC J Res.* 2025;12(1):1–17.  
doi: 10.1177/24723444241303970
19. Boumegnane A, Nadi A, Cochrane C, *et al.* Formulation of conductive inks printable on textiles for electronic applications: A review. *Text Prog.* 2022;54(2):103–200.  
doi: 10.1080/00405167.2021.2094135
20. Camargo JR, Orzari LO, Araújo DAG, *et al.* Development of conductive inks for electrochemical sensors and biosensors. *Microchem J.* 2021;164:105998.  
<https://doi.org/10.1016/j.microc.2021.105998>
21. Kholuiskaya SN, Siracusa V, Mukhametova GM, *et al.* An approach to a silver conductive ink for inkjet printer technology. *Polymers.* 2024;16(12):1731.  
doi: 10.3390/polym16121731
22. Saidina DS, Eawwiboonthanakit N, Mariatti M, *et al.* Recent development of graphene-based ink and other conductive material-based inks for flexible electronics. *J Electron Mater.* 2019;48(6):3428–50.  
<https://doi.org/10.1007/s11664-019-07183-w>
23. Yaqoob AA, Umar K, Ibrahim MNM. Silver nanoparticles: Various methods of synthesis, size affecting factors and their potential applications—A review. *Appl Nanosci.* 2020;10:1369–78.  
doi: 10.1007/s13204-020-01318-w
24. Htwe YZN, Mariatti M. Performance of water-based printed hybrid graphene/silver nanoparticle conductive inks for flexible strain sensor applications. *Synth Met.* 2023;300:117495.  
<https://doi.org/10.1016/j.synthmet.2023.117495>
25. Phillips C, Al-Ahmadi A, Potts SJ, *et al.* The effect of graphite and carbon black ratios on conductive ink performance. *J Mater Sci.* 2017;52:9520–30.  
doi: 10.1007/s10853-017-1114-6
26. Saidina DS, Mariatti M, Zubir SA, *et al.* Performance of graphene hybrid based ink for flexible electronics. *J Mater Sci Mater Electron.* 2019;30:19906–16.  
doi: 10.1007/s10854-019-02357-y
27. Liu L, Zhang Y, Wu H, *et al.* Highly conductive graphene/carbon black screen-printing inks for flexible electronics. *J Colloid Interface Sci.* 2021;582:12–21.  
doi: 10.1016/j.jcis.2020.07.106
28. Htwe YZN, Ismail NH, Jaafar M. Performance of inkjet-printed strain sensor based on graphene/silver nanoparticles hybrid conductive inks on polyvinyl alcohol substrate. *J Mater Sci Mater Electron.* 2020;31:15361–71.  
doi: 10.1007/s10854-020-04100-4
29. Kwon YJ, Kim Y, Jeon H, *et al.* Graphene/carbon nanotube hybrid as a multi-functional interfacial reinforcement for carbon fiber-reinforced composites. *Compos Part B Eng.* 2017;122:23–30.  
doi: 10.1016/j.compositesb.2017.04.005
30. Xu LY, Yang GY, Jing HY, *et al.* Ag-graphene hybrid conductive ink for writing electronics. *Nanotech.* 2014;25(5):055201.  
doi: 10.1088/0957-4484/25/5/055201
31. Hong Z, Zheng Z, Kong L, *et al.* Welded carbon nanotube-graphene hybrids with tunable strain sensing behavior for wide-range bio-signal monitoring. *Polymers.* 2024;16:238.  
doi: 10.3390/polym16020238
32. Wang J, Li L, Liu H, *et al.* Graphene/carbon nanotube conductive ink-based biomimetic structure for self-powered flexible medical monitoring devices. *ACS Appl Nano Mater.* 2024;7(2):1863–75.  
doi: 10.1021/acsanm.3c05095

33. Htwe YZN, Mariatti M. Printed graphene and hybrid conductive inks for flexible, stretchable and wearable electronics: Progress, opportunities and challenges. *J Sci Adv Mater Devices*. 2022;7:100435. <https://doi.org/10.1016/j.jsamd.2022.100435>
34. Stanciu NV, Stan F, Fetecau C. Experimental investigation of the melt shear viscosity, specific volume and thermal conductivity of low-density polyethylene/multi-walled carbon nanotube composites using capillary flow. *Polymers*. 2020;12(6):1230. <https://doi.org/10.3390/polym12061230>
35. Subad R, Ishraaq R, Dasgupta A, *et al.* Development of highly conductive and stable direct writeable metal-free inks based on carbon nanotube and functionalized graphene oxide. *ACS Appl Mater Interfaces*. 2025;17(31):45056–65. doi: 10.1021/acsmi.5c07337
36. Dave P, Rajani A. Review on carbon-graphene nanocomposite based conductive ink in printed electronics. *Int J Adv Nano Comput Anal*. 2021;1(1):61–83. doi: 10.61797/ijanca.v1i1.89
37. Hairi NIIM, Md Ralib AA, Nordin AN, *et al.* Recent advance in using eco-friendly carbon-based conductive ink for printed strain sensor: A review. *Cleaner Mater*. 2024;12:100248. <https://doi.org/10.1016/j.clema.2024.100248>
38. Akindoyo JO, Ismail NH, Mariatti M. Development of environmentally friendly inkjet printable carbon nanotube-based conductive ink for flexible sensors: Effects of concentration and functionalization. *J Mater Sci Mater Electron*. 2021;32(9):12648–60. doi: 10.1007/s10854-021-05900-y
39. Qin Y, Ouyang X, Lv Y, *et al.* A review of carbon-based conductive inks and their printing technologies for integrated circuits. *Coatings*. 2023;13:1769. doi: 10.3390/coatings13101769
40. Dey A, Kalita AJ, Khatun H, *et al.* The development of an affordable graphite-based conductive ink for printed electronics. *Eng Proc*. 2025;87:17. doi: 10.3390/engproc2025087017
41. Zappi D, Varani G, Cozzoni E, *et al.* Innovative eco-friendly conductive ink based on carbonized lignin for the production of flexible and stretchable biosensors. *Nanomaterials*. 2021;11:3428. doi: 10.3390/nano11123428
42. Chaleawlerlert-umpon S, Liedel C. More sustainable energy storage: Lignin-based electrodes with glyoxal crosslinking. *J Mater Chem A*. 2017;5:24344–52. <https://doi.org/10.1039/C7TA07686J>
43. Sýs M, Khaled E, Metelka R, *et al.* Electrochemical characterisation of novel screen-printed carbon paste electrodes for voltammetric measurements. *J Serb zChem Soc*. 2017;82:865–77. <https://doi.org/10.2298/JSC170207048S>
44. Nag A, Mitra A, Mukhopadhyay SC. Graphene and its sensor-based applications: A review. *Sens Actuators A Phys*. 2018;270:177–94. doi: 10.1016/j.sna.2017.12.028
45. Prolongo SG, Moriche R, Jimenez-Suarez A, *et al.* Advantages and disadvantages of the addition of graphene nanoplatelets to epoxy resins. *Eur Polym J*. 2014;61:206–14. doi: 10.1016/j.eurpolymj.2014.09.022
46. Irani FS, Shafaghi AH, Tasdelen MC, *et al.* Graphene as a piezoresistive material in strain sensing applications. *Micromachine*. 2022;13(1):119. <https://doi.org/10.3390/mi13010119>
47. Kumari L, Zhang T, Du GH, *et al.* Synthesis, microstructure and electrical conductivity of carbon nanotube-alumina nanocomposites. *Ceramic Int*. 2009;35:1775–81. doi: 10.1016/j.ceramint.2008.10.005
48. Karagiannidis PG, Hodge SA, Lombardi L. Microfluidization of graphite and formulation of graphene-based conductive inks. *ACS Nano*. 2016;11(3):2742–55. doi: 10.1021/acsnano.6b07735

**How to Cite:** Mishra JK, Francis V. Development of Sustainable CNT-Polymer Conductive Ink. *Int Res J Multidiscip Scope*. 2026; 2026; 7(2): 78-95. DOI: 10.47857/irjms.2026.v07i02.08821